THE JOURNAL OF BIOLOGICAL CHEMISTRY
Vol. 278, No. 45, Issue of November 7, pp. 44874–44885, 2003
Printed in U.S.A.

Cloning and Developmental Analysis of Murid Spermatid-specific Thioredoxin-2 (SPTRX-2), a Novel Sperm Fibrous Sheath Protein and Autoantigen*

Received for publication, May 24, 2003, and in revised form, July 9, 2003
Published, JBC Papers in Press, August 7, 2003, DOI 10.1074/jbc.M305475200

Antonio Miranda-Vizuete,[a,b] Katie Tsang,[c] Yang Yu,[c] Alberto Jiménez,[a,d] Markku Pelto-Huikko,[e,f] Charles J. Flickinger,[g,h] Peter Sutovsky,[i,j] and Richard Oko[b,c,k]

From the [a]Center for Biotechnology, Department of Biosciences at Novum, Karolinska Institutet, S-14157 Huddinge, Sweden, the [c]Department of Anatomy and Cell Biology, Queen's University, Kingston, Ontario K7L 3N6, Canada, the [e]Department of Developmental Biology, Tampere University Medical School, and the Department of Pathology, Tampere University Hospital, Fin-33101 Tampere, Finland, the [g]Department of Cell Biology, University of Virginia, Charlottesville, Virginia 22908, and the [i]Departments of Animal Science and Obstetrics and Gynecology, University of Missouri, Columbia, Missouri 65211-5300

Thioredoxins compose a growing family of proteins that participate in different cellular processes via redox-mediated reactions. We report here the cloning, developmental expression, and location of murid *Sptrx-2*. Mouse and rat SPTRX-2 proteins display a high homology to their human ortholog in the thioredoxin and NDP kinase domains, and the coding genes are located at syntenic positions. Northern blotting and *in situ* hybridization confirmed the testis-specific expression of murine *Sptrx-2* mRNA, mostly in round spermatids. Immunohistochemical analysis of the 19 steps of rat spermiogenesis showed that SPTRX-2 expression becomes prominent in the cytoplasmic lobe of step 15–18 spermatids and diminishes in step 19 just before spermiation. However, in the spermatid tail, SPTRX-2 immunoreactivity increased from step 15 to 19 and was confined to the principal piece. By immunogold electron microscopy, SPTRX-2 was first detected scattered throughout the cytoplasm of the axoneme in step 14–15 spermatids, but began to be incorporated by step 16 into the fibrous sheath (FS). During steps 17–18, the labeling increased over the ribs and columns of the assembled FS. It peaked in step 19 and remained in the FS of epididymal spermatozoa. Immunoblots of isolated FS obtained from spermatozoa confirmed that SPTRX-2 is an integral component of the FS and a post-obstruction autoantigen in vasectomized rats. Our data indicate that SPTRX-2 incorporation into the FS lags well behind FS assembly, suggesting it is required during the final stages of sperm tail maturation in the testis and/or epididymis, where extensive disulfide bonding of FS proteins occurs.

Thioredoxins are a class of multifunctional proteins that participate in a variety of redox reactions by the reversible oxidation of the cysteine residues in their conserved active-site Cys-Gly-Pro-Cys (1). Based on this active-site sequence, seven thioredoxin proteins in humans have been reported to date. Four members of the family are found ubiquitously expressed in all tissues within the same organism and are composed of either thioredoxin domains alone (TRX-1 and TRX-2) or thioredoxin fusions with other protein domains (TXL-1 and ERDJ5): TRX-1, a cytosolic enzyme that can translocate into the nucleus upon certain stimuli (2); TRX-2, a mitochondrial protein (3); TXL-1/TRP32, a cytosolic enzyme of unknown function (4, 5); and ERDJ5, an endoplasmic reticulum resident protein also belonging to the DnaJ/Hsp40 chaperone family (6, 7). In addition, two tissue-specific testicular thioredoxins named SPTRX-1 and SPTRX-2 have been recently reported in the tail of spermatozoa (8, 9), and another member named TXL-2 has been found in tissues harboring cilia and flagella and shown to have microtubule-binding activity (10). The number of functions assigned to the different thioredoxins is increasing proportionally to the number of new members of the family being discovered. For example, thioredoxins are electron donors for essential enzymes such as ribonucleotide reductase, regulators of transcription factor DNA-binding activity, modulators of apoptosis and antioxidant defense, and participants in the regulation of the protein folding process (reviewed in Refs. 1, 11, and 12).

The primary function of the spermatozoon is to contribute the paternal half of chromosomes to the offspring. In higher vertebrates, the complexity of the fertilization process is increased by the advent of internal fertilization and by the functional adaptations of the oocyte vestments. To circumvent these hurdles, the spermatozoon has acquired a highly specialized morphology comprising cytoskeletal components, which appear to have no structural counterpart in somatic cells. The most evident among these cytoskeletal structures are the perinuclear theca of the sperm head and the outer dense fibers

* This work was supported in part by grants from the Canadian Institutes of Health Research and National Sciences and Engineering Research Council of Canada (to R. O.) and by Swedish Medical Research Council Projects 03P-14096, 03X-14041, and 13X-10370 and grants from the Åke Wibergs Stiftelse and the Karolinska Institutet (to A. M.-V.). The costs of publication of this article were defrayed in part by the payment of page charges. This article must therefore be hereby marked "*advertisement*" in accordance with 18 U.S.C. Section 1734 solely to indicate this fact.

The nucleotide sequence(s) reported in this paper has been submitted to the GenBank™/EBI Data Bank with accession number(s) AF548543 and AF548544.

[b] Both authors contributed equally to this work.

[d] Supported by the Fundación Margit and Folke Pehrzon.

[f] Supported by the Research Fund of the Tampere University Hospital, Tampere University.

[h] Supported by NIDDK Grant P50 DK45179 and NICHD Grant HD U54-29009 from the National Institutes of Health.

[j] Supported by the Food for the 21st Century Program of the University of Missouri, United States Department of Agriculture Grants 2002-02069 and 99-35203-7785, and National Institute for Occupational Safety and Health Grant OH07324-01.

[k] To whom correspondence should be addressed. Tel.: 613-533-2858; Fax: 613-533-2566; E-mail: ro3@post.queensu.ca.

(ODFs)[1] and fibrous sheath (FS) of the sperm tail (13–15). The perinuclear theca is a condensed layer of selected cytoplasmic proteins that are sandwiched between the nuclear envelope and the inner acrosomal membrane apically and between the nuclear envelope and the plasma membrane caudally. It is assumed to play a pivotal role in acrosomal-nuclear docking, nuclear shaping, and sperm-oocyte interactions (16, 17). ODFs surround the axoneme in the middle and principal pieces of the sperm tail. In the middle piece, nine ODFs associate with the corresponding microtubule doublets of the axoneme, whereas in the principal piece, ODF3 and ODF8 are fused to the two longitudinal columns of the FS, which are bridged by FS ribs and together surround the seven remaining ODFs (14, 18).

The function of the ODFs and FS is not fully elucidated, but it seems to be related to the control of flagellar motility (13, 19) and protection against shearing forces during epididymal transit (20). However, evidence for an active rather than a merely structural role of the ODFs and FS in sperm function is increasing, supported by the fact that, among their constituent proteins, there are several molecules displaying either enzymatic or regulatory functions. For example, in the FS, glyceraldehyde 3-phosphate dehydrogenase produces ATP via the glycolytic pathway. This is critical for the transition to hyperactivated motility as well as capacitation (21). Moreover, the initiation and maintenance of sperm motility are regulated by a cascade of phosphorylation/dephosphorylation events (reviewed in Ref. 22). In this respect, AKAP82 (A kinase-anchoring protein of 82 kDa), also located in the FS, presumably tethers cAMP-dependent protein kinase A, directing and specifying the actions of the kinase in close proximity to the sperm's axonemal machinery (reviewed in Ref. 23). Both the ODFs and FS are composed of many different polypeptides, of which only a few have been cloned and characterized to date. ODF1 (also known as RT7 and ODF27) (24–26), ODF2 (also named ODF84) (27–29), ODF3 (30), TPX-1 (31), and SAK57 (32) are among the characterized ODF proteins. A similar number of FS proteins have been described in mammalian spermatozoa: AKAP4 (also named p82, FSC1, and FS75) (33–38), AKAP3 (FS95) (37–39), TAKAP80 (40), glutathione *S*-transferase (41), glyceraldehyde 3-phosphate dehydrogenase-S (42), type I hexokinase (43), ropporin (44), rhophilin (45), FS39 (46), and CABYR (47). In addition, some other proteins found in the sperm tail, such as SHIPPO1 and OPPO1 (48, 49), may contribute to the molecular makeup of the FS and ODFs.

In this context, we have recently described the identification and characterization of SPTRX-1 (spermatid-specific thioredoxin-1), a novel member of the thioredoxin family of proteins that transiently associates with the longitudinal columns of the FS during sperm tail assembly (8, 50). A second member of the thioredoxin family named SPTRX-2 has also been identified in the human sperm tail and is composed of an N-terminal thioredoxin domain followed by three NDP kinase domains (9). We report here the cloning of mouse and rat *Sptrx-2*, their patterns of development during spermiogenesis, and their exact localizations within the sperm tail. SPTRX-2 incorporates into both the ribs and longitudinal columns of the FS in the last steps of spermatid development and remains as an integral FS component in mature epididymal spermatozoa. Its expression pattern contrasts with the transient nature of SPTRX-1 expression during FS formation (50). Finally, we identify SPTRX-2 as a novel sperm autoantigen after vasectomy.

[1] The abbreviations used are: ODFs, outer dense fibers; FS, fibrous sheath; TRITC, tetramethylrhodamine isothiocyanate; contig, group of overlapping clones.

MATERIALS AND METHODS

Cloning of Mouse and Rat Sptrx-2 cDNAs—BLAST (51) was used to perform a survey of different data bases at NCBI[2] to identify entries encoding the potential mouse and rat orthologs of human *SPTRX-2* (9). Using this strategy, we found the expressed sequence tag entries BQ839895 and BB573861 to partially code for the putative mouse *Sptrx-2* sequence. Based on these sequences, we designed nested forward and reverse primers that were used for 5′- and 3′-rapid amplification of cDNA ends of a mouse testis cDNA library (Clontech). The resulting sequences were used to amplify by PCR the full-length cDNA of mouse *Sptrx-2* from the same library. The amplification product was cloned in the pGEM-Teasy vector (Promega) and sequenced in both directions. For the rat ortholog, the same strategy was followed using mouse *Sptrx-2* sequence and a BLAST search against the rat trace archive.[3] This search strategy rendered several potential rat sequences that were used to design specific primers at the putative translation initiation and stop codons and to amplify by PCR the rat *Sptrx-2* open reading frame from a rat testis cDNA library (Clontech).

Northern Blot Analysis and in Situ Hybridization—A mouse multiple-tissue Northern blot and mouse RNA Master blots with poly(A)$^+$ RNA from different tissues were purchased from Clontech. The mouse *Sptrx-2* open reading frame was labeled with [α-^{32}P]dCTP (Rediprime random primer labeling kit, Amersham Biosciences) and hybridized at 60 °C overnight in Ultrahyb™ solution following the protocol provided by Ambion Inc. The blot was also hybridized with mouse β-actin as a control. The blots were scanned and quantified with the Gel Pro Analyzer program (Media Cybernetics). For *in situ* hybridization, mouse and rat testes were frozen on dry ice, sectioned with a Microm HM500 cryostat at 14 μm, and thaw-mounted onto Polylysine glass slides (Menzel). The sections were stored at −20 °C until used. Four different probes (based on mouse and rat *Sptrx-2* cDNA sequences, respectively) were used. Because all produced similar results when used separately, they were usually used simultaneously to intensify the signal. Several control probes with the same length and similar GC content and specific activity were used to determine the specificity of the hybridization. *In situ* hybridization was carried out as described previously (52).

Production of Recombinant SPTRX-2 Protein and Affinity-purified Antibodies—The open reading frame encoding human *SPTRX-2* was cloned into the *Bam*HI-*Eco*RI sites of the pGEX-4T-1 expression vector (Amersham Biosciences) and used to transform *Escherichia coli* BL21(DE3). A single positive colony was inoculated in 1 liter of LB medium plus ampicillin and grown at 37 °C to A_{600} = 0.5. The production and purification of the fusion protein were performed as described previously (9). Protein concentration was determined from the absorbance at 280 nm using a molar extinction coefficient of 47,330 M^{-1} cm^{-1}.

Purified glutathione *S*-transferase-human SPTRX-2 was used to immunize rabbits (Zeneca Research Biochemicals). After six immunizations, sera from rabbits were purified by ammonium sulfate precipitation. Affinity-purified antibodies were prepared using a cyanogen bromide-activated Sepharose 4B column (Amersham Biosciences) to which 0.5 mg of recombinant SPTRX-2 had been coupled using the procedure recommended by the manufacturer. Antibody specificity was tested by Western blotting using recombinant SPTRX-2 and testicular cell extracts.

Mouse/Rat Testicular and Epididymal Sample Preparation, Immunocytochemistry, and Electron Microscopy—Adult male Sprague-Dawley rats and CD-1 mice were anesthetized, and the testes and epididymides were fixed by perfusion through the abdominal aorta and heart, respectively, with 0.8% glutaraldehyde and 4% paraformaldehyde in 0.1 M phosphate buffer containing 50 mM lysine (pH 7.4), with 4% paraformaldehyde (mice only), or in Bouin's fixative (for light microscopy). Tissues destined for Lowicryl (SPI Supplies, West Chester, PA) or LR White (Polysciences, Inc., Warrington, PA) embedding (for electron microscopy) were immersed in the respective fixatives for 2 h at 4 °C, washed three times with phosphate buffer, and incubated with phosphate buffer containing 50 mM NH_4Cl for 1 h at 4 °C. Tissues were subsequently washed with buffer, dehydrated in graded methanol up to 90%, and infiltrated and embedded in Lowicryl K4M or LR White. Thin sections were mounted on Formvar-coated nickel grids for immunogold labeling. Rat and mouse tissues fixed in Bouin's fixative were washed extensively with 75% alcohol before being completely dehydrated in ethanol and embedded in paraffin. For light microscopic immunocytochemistry, 5-μm paraffin sections were deparaffinized and hydrated through a graded series of ethanol concentrations before immunoper-

[2] Available at www.ncbi.nlm.nih.gov/.

[3] Available at www.ncbi.nlm.nih.gov/Traces/trace.cgi.

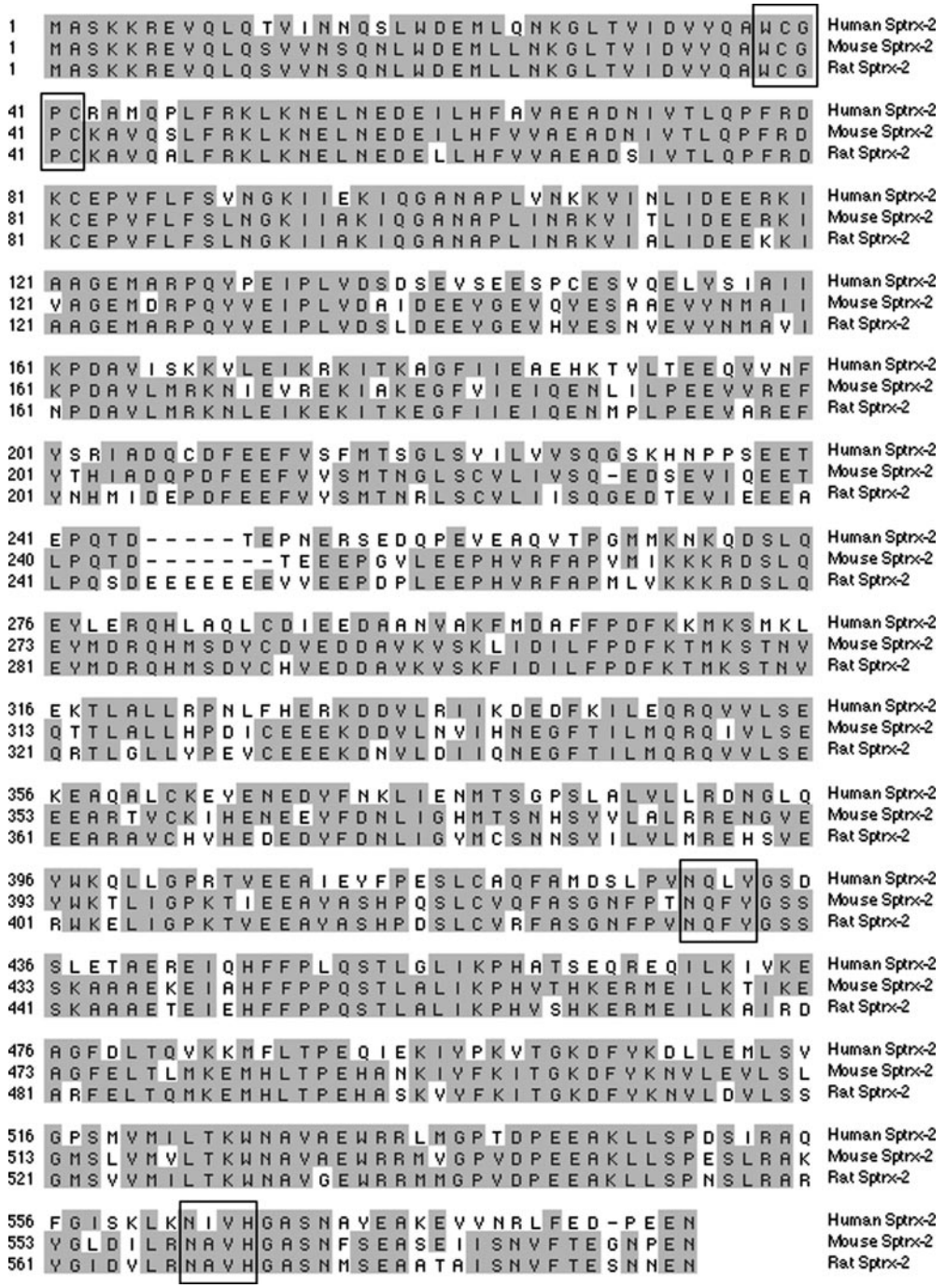

FIG. 1. **Alignment of the predicted amino acid sequences of the human, mouse, and rat SPTRX-2 proteins.** Alignment was performed using the ClustalW program included in the DNAStart package (75). Identical residues are *shaded*, and the thioredoxin and NDP kinase active sites are *boxed*.

oxidase localization with anti-SPTRX-1 antibody by standard procedures (14). For electron microscopic immunocytochemistry, ultrathin Lowicryl or LR White sections on Formvar-coated nickel grids were immunogold-labeled according to the procedure of Oko *et al.* (53). Staging of the cycle of the seminiferous epithelium and determining the steps of spermiogenesis were done according to the classifications of Leblond and Clermont (54).

For immunofluorescence, mouse testes were isolated, cut into small pieces ($5 \times 5 \times 5$ mm), and fixed by immersion in 4% paraformaldehyde. After vigorous repeated washing with phosphate-buffered saline and sucrose, the tissues were embedded in paraffin using conventional histochemical techniques and sectioned. Four-millimeter-thick sections were mounted on slides, dewaxed by xylene and ethanol changes, treated for autofluorescence reduction in 1% picric acid in a steamer, and blocked for 30 min in 5% normal goat serum (Sigma) in phosphate-buffered saline. In the same trials, mouse epididymides were removed, and the spermatozoa were released by gentle mincing into Tyrode's albumin lactate pyruvate/HEPES medium. Spermatozoa were collected by a 5-min centrifugation at $350 \times g$ and attached to poly-L-lysine-coated coverslips (22×22 mm). A labeling solution composed of phosphate-buffered saline with 1% normal goat serum and 0.1% Triton X-100 was used for antibody dilutions, incubations, and washes.

Immunofluorescence processing of paraffin sections was performed on a histology tray under humid and dark conditions. Samples were first incubated for 40 min with anti-SPTRX-2 serum (diluted 1:100) and then washed by submersion for 5 min and incubated with a mixture of red fluorescent TRITC-labeled goat anti-rabbit IgG (diluted 1:80; Zymed Laboratories Inc., South San Francisco, CA) and 2.5 μg/ml 4,6-diamidino-2-phenylindole (Molecular Probes, Inc. Eugene, OR). After washing, the samples were mounted on slides (whole mounted spermatozoa on coverslips) or covered with coverslips (tissue sections on slides) in Vectashield mounting medium (Vector Labs, Inc.). Negative

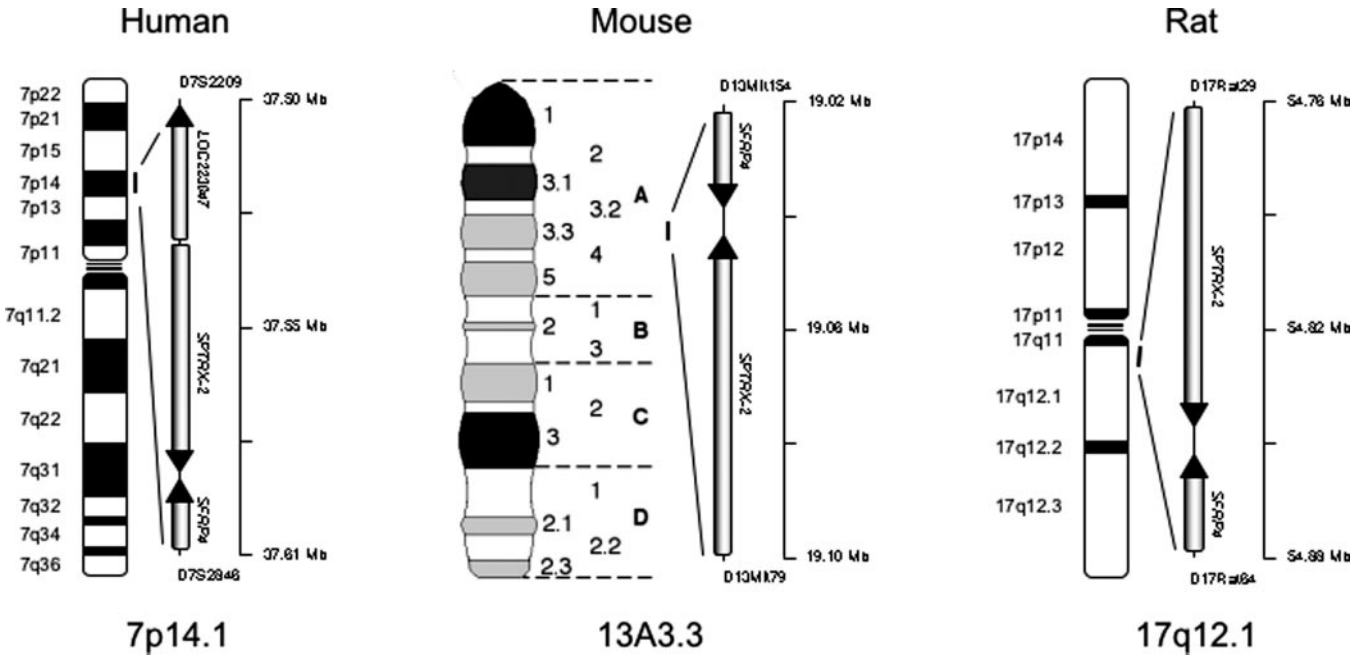

FIG. 2. **Chromosomal localization of the mammalian *Sptrx-2* orthologs.** The human *SPTRX-2* gene is located between markers D7S2209 and D7S2846 at 58.84–59.12 centimorgams from the top of the linkage group of human chromosome 7 (based on the deCODE high resolution recombination map of the human genome (76)). By comparing this location with other genes in the region, we have mapped the human *SPTRX-2* gene to chromosome 7p14.1 flanked by the genes *LOC223047* and *SFRP4*. The mouse *Sptrx-2* gene maps between markers D13Mit154 and D13Mit79 at 11.0–12.0 centimorgans from the top of the linkage group of mouse chromosome 13, in a region syntenic to that of human chromosome 7p14.1 (Whitehead Institute/Massachusetts Institute of Technology, Center for Genome Research, Database Release 1999 at www.informatics.jax.org). By comparing this location with the mouse *Sfrp4* gene (60), we have mapped the mouse *Sptrx-2* gene to chromosome 13A3.3. The rat *Sptrx-2* gene maps between markers D17Rat29 and D17Rat64 at 38.87–39.69 centimorgans from the top of the linkage group of rat chromosome 17, also in a region syntenic to that of human chromosome 7p14.1. By comparing this location with the rat *Sfrp4* gene, we have mapped the rat *Sptrx-2* gene to chromosome 17q12.1. *Mb*, megabases.

controls were performed by the replacement of the first antibody with nonimmune rabbit serum or with anti-SPTRX-2 serum saturated with recombinant SPTRX-2. Samples were examined in a Nikon Eclipse 800 microscope. Images were captured with a CoolSnap HQ RTE/CCD 1217 digital camera using MetaMorph software.

Western Blot Analysis of Sperm Autoantibodies and the FS—Adult male Lewis rats (225–275 g; Charles River Laboratories, Wilmington, MA) received a bilateral vasectomy as described previously (55). Sera were collected prior to vasectomy and 3 months after the operation. Sperm were prepared from Lewis rat cauda epididymides by back-flushing fluid through the vas deferens (55).

For two-dimensional gel electrophoresis, sperm were pelleted by centrifugation and solubilized in sample buffer containing 7 M urea, 2 M thiourea, 0.2% Nonidet P-40, 100 mM dithiothreitol, and 0.2% pH 3.5–10 Ampholine (Amersham Biosciences). Aliquots of the extracts containing 150–200 μg of protein were applied to a Protean IEF cell (Bio-Rad) with pH 3–10 immobilized pH gradient strips for the first dimension isoelectric focusing. After active rehydration of immobilized pH gradient strips with sample buffer at 50 V, they were focused at 250 V for 15 min and stepped up to 8000 V until 30,000 total V-h were reached (~6 h). SDS-PAGE on 8–15% gels in the second dimension was performed as described previously (56), and proteins were stained on the gels with Coomassie Blue or were electroblotted onto nitrocellulose membranes (56). For Western blot analysis, membranes containing sperm proteins were washed and blocked with milk. Primary pre- or post-obstruction sera (diluted 1:250) were incubated with the membranes overnight at 4 °C and exposed to the secondary antibody (diluted 1:5000), horseradish peroxidase-conjugated goat anti-rat IgG (Jackson ImmunoResearch Laboratories, Inc., West Grove, PA). Other two-dimensional blots of sperm proteins were incubated with a 1:25,000 dilution of affinity-purified rabbit antiserum raised against recombinant SPTRX-2. These blots were subsequently exposed to horseradish peroxidase-conjugated goat anti-rabbit IgG (diluted 1:5000), washed, and treated with the peroxidase substrate 3,3′,5,5′-tetramethylbenzidine and 0.01% H_2O_2 (Kirkegaard & Perry Laboratories, Gaithersburg, MD).

For one-dimensional Western blots of recombinant SPTRX-2, the protein was solubilized in Laemmli buffer (57). Three micrograms of protein were loaded per lane for staining with post-vasectomy serum, and 50 ng were loaded per lane for use with anti-SPTRX-2 serum. SDS-PAGE was conducted as described previously (58); and after transfer to nitrocellulose, the membranes were exposed to post-vasectomy rat serum (diluted 1:250) or to anti-SPTRX-2 serum (diluted 1:100,000), followed by the appropriate secondary antibody and development of the reaction product as described for two-dimensional analysis. Controls consisted of pre-vasectomy rat serum, preimmune rabbit serum (for anti-SPTRX-2 antibody), and omission of the postvasectomy serum. Isolation procedures, SDS-PAGE (under reduced conditions), Western blotting, and immunoblotting of sperm head and tail fractions including the FS were done as described by Yu *et al.* (50).

RESULTS

cDNA Cloning, Sequence Analysis, Genomic Organization, and Chromosomal Localization of the Mouse and Rat Sptrx-2 Genes—By sequence comparison with human *SPTRX-2* (9), we found several GenBank™/EBI mouse-expressed sequence tag entries that, when translated, displayed high homology to the human ortholog. Therefore, we designed specific primers based on these sequences and performed 5′- and 3′-rapid amplification of cDNA ends/PCR analysis using a mouse testis cDNA library to clone the full-length mouse *Sptrx-2* cDNA. An identical strategy was followed to identify the rat ortholog using the rat trace archive and a rat testis cDNA library. Both mouse and rat *Sptrx-2* cDNAs encode very similar proteins of 586 and 595 amino acids with calculated molecular masses of 66.9 and 68.1 kDa, respectively. A comparison of these two proteins with human SPTRX-2 (9) shows a high degree of homology among the three orthologs, which are organized into two distinct domains: an N-terminal domain (comprising the first 105 residues) similar to thioredoxins and a C-terminal domain composed of three (one incomplete and two complete) tandem-repeated NDP kinase domains (Fig. 1). The major differences are located in the incomplete first NDP kinase domain, where the rat protein has a stretch of glutamine residues not present in either the human or mouse ortholog and the function of which remains unknown. As inferred from Fig. 1, the amino

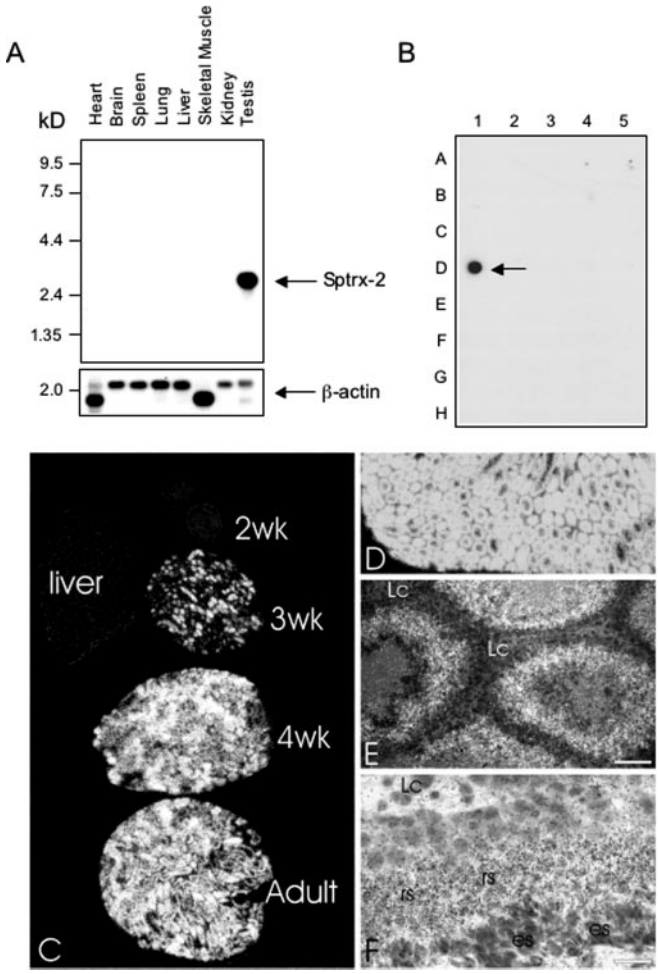

FIG. 3. **Expression pattern of mouse *Sptrx-2* mRNA.** *A*, mouse multiple-tissue Northern blot. The mouse *Sptrx-2* probe hybridized with one mRNA species at 2.5 kb only in the testis. β-Actin was used as control. *B*, shown is the mouse mRNA master blot in which the *Sptrx-2* probe hybridized only with testicular mRNA (*arrow*) (for a complete list of mouse tissues, see www.clontech.com/archive/OCT97UPD/MasterBlot.shtml). *C*, *in situ* hybridization in mouse testicular sections studied at different ages shows the presence of *Sptrx-2* mRNA in the testes from 3-week (*wk*)-old to adult mice, but not in pre-pubertal testis (2-week-old) or liver used as negative control tissues. *D*, in rat testis, all seminiferous tubules exhibited a strong signal for *Sptrx-2* mRNA. *E*, in dipped sections of adult mouse testis, the strongest signal (epipolarization signal seen as *white grains*) can be identified in the middle part of the seminiferous epithelium, whereas the rest of the tubule and labeling of the interstitial Leydig cells (*Lc*) did not exceed background levels. *Bar* = 50 μm. *F*, at higher magnification, round spermatids (*rs*) showed a strong signal, whereas elongating spermatids (*es*) and early spermatogenic cells and Leydig cells exhibited only background labeling. *Bar* = 20 μm.

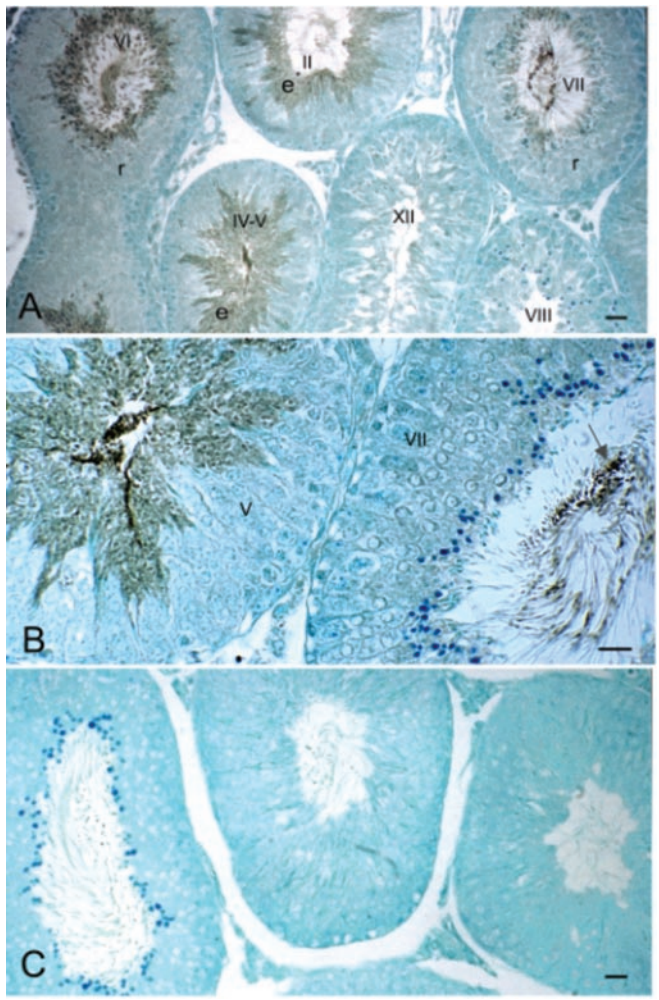

FIG. 4. **Expression pattern of mouse SPTRX-2 protein.** *A*, shown is a low magnification view of a paraffin section of rat seminiferous epithelium immunoperoxidase-stained with affinity-purified anti-SPTRX-2 antibody (diluted 1:250). Immunoperoxidase staining (*brown* precipitate) was most evident in the elongated spermatid layer (*e*) of the seminiferous epithelium, whereas staining in the cytoplasm of round spermatids (*r*) was barely detectable. Cytoplasmic immunoreactivity was prominent in step 15–18 spermatids (stages I–VI), but diminished in step 19 spermatids (stages VII and VIII). Sperm tail immunoreactivity became detectable in steps 15 and 16 (stages I and II) and gradually increased in intensity until step 18 and 19 spermatids (stages VI–VIII). *Bar* = 20 μm. *B*, shown is a higher magnification section of rat testis immunoperoxidase-stained with anti-SPTRX-2 antibody. Immunostaining was strong in the tails of elongated spermatids from late step 17 to step 19 (stages V–VIII). It is evident that tails in step 19 were strongly stained at their distal end (*arrow*). *Bar* = 10 μm. *C*, in rat seminiferous epithelium, no immunoreactivity was detectable when anti-SPTRX-2 antibody was preincubated with recombinant SPTRX-2 prior to staining. *Bar* = 10 μm.

acid identity among the three orthologs is higher in the N-terminal thioredoxin domain than in the NDP kinase domains. All of the structural amino acids that are conserved in previously characterized mammalian thioredoxins (including human SPTRX-2) are also conserved in mouse and rat SPTRX-2, including those residues shown to be essential for catalysis, maintenance of three-dimensional structure, or protein-protein interactions such as Asp-26, Trp-31, Pro-75, and Gly-91 (numbers refer to positions in human TRX-1). Consistent with this, the typical thioredoxin active site (WCGPC) is conserved among the three proteins, whereas the active sites of the last two NDP kinase domains in mouse and rat differ from that of the human counterpart. Thus, whereas the sequence of the active sites of the two complete NDP kinase domains are NQLY and NIVH in human SPTRX-2 (9), these sequences are altered to NQFY and NAVH in mouse and rat, respectively.

A comparison of the mouse and rat SPTRX-2 protein sequences with the PROSITE Database (59) identified, along with the above-mentioned thioredoxin and NDP kinase domains, several potential phosphorylation sites and a PEST sequence for ubiquitin/proteasome-dependent degradation centered at residue 242. This result is identical to that obtained with human SPTRX-2 and supports a common regulatory mechanism for the three orthologs.

To determine the genomic organization, the mouse and rat *Sptrx-2* cDNA sequences were BLAST-searched against their respective data bases at NCBI. The results obtained indicate that the mouse *Sptrx-2* gene is present in the supercontig

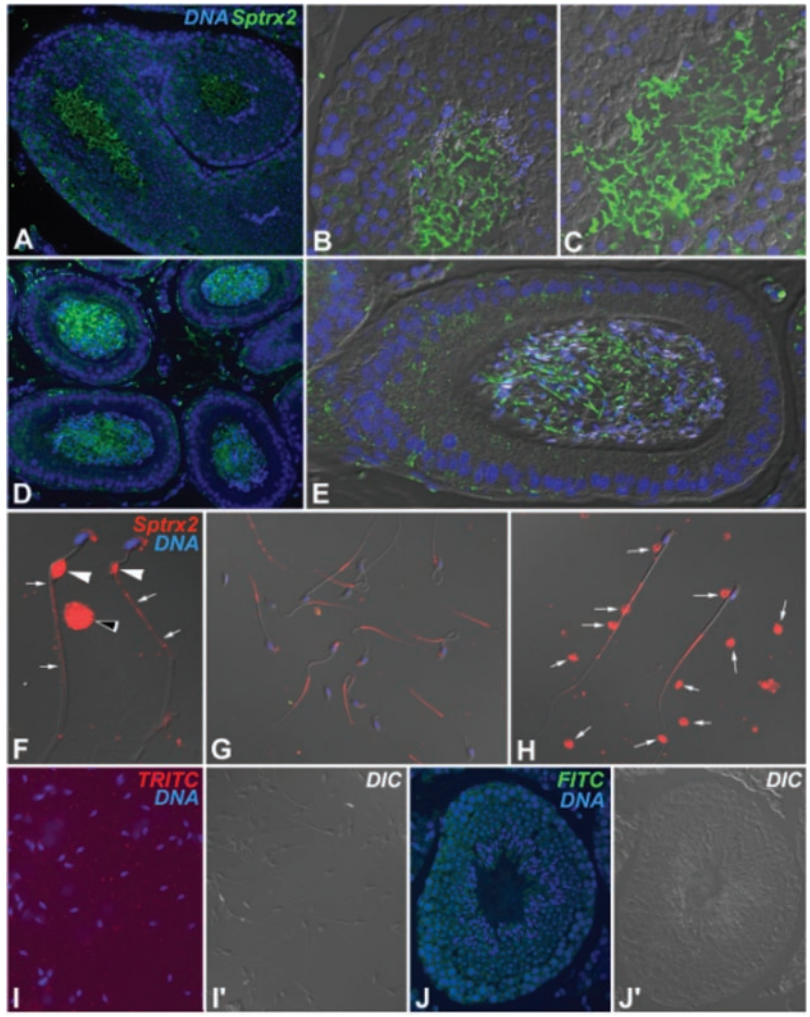

FIG. 5. **Immunofluorescence of mouse SPTRX-2 on testicular (*A–C*, *J*, and *J′*) and epididymal (*D* and *E*) tissue sections and in isolated testicular (*F*) and epididymal (*G–I* and *I′*) spermatozoa.** *A–C*, in the testis, SPTRX-2 (*green*) is located near the lumen of seminiferous tubules, corresponding to the elongated spermatids and fully differentiated spermatozoa. *D* and *E*, SPTRX-2 in the epididymis is confined to the principal piece of the tails of spermatozoa collected in the epididymal lumen. Autofluorescence of the basal lamina of the epididymal tubules is visible in *D*. *F*, residual bodies (*black arrowhead*), distal cytoplasmic droplets (*white arrowheads*), and the testicular sperm tail principal pieces (*arrows*) display intense anti-SPTRX-2 antibody immunoreactivity (*red*). *G* and *H*, SPTRX-2 (*red*) is mainly present in the sperm tail principal piece and in the detached cytoplasmic droplets (*arrows* in *H*) isolated from mouse epididymis. *I* and *I′*, shown are epifluorescence (*I*) and differential interference contrast (*DIC*; *I′*) views of the negative control, cauda epididymal spermatozoa processed with the recombinant protein-saturated anti-SPTRX-2 serum and red fluorescent goat anti-rabbit IgG. *J* and *J′*, shown are the results from a similar negative control performed on testicular tissue sections. DNA in all images was counterstained with the blue fluorescent DNA-binding probe 4,6-diamidino-2-phenylindole. The epifluorescence signals in *B*, *C*, and *E–H* were superimposed over the differential interference contrast images acquired in the same focal planes. *FITC*, fluorescein isothiocyanate.

NT_039578 and that the rat *Sptrx-2* gene is found in the supercontig NW_043107; and in both cases, the genomic organization is identical to that of the reported human *SPTRX-2* gene (9), being composed of 17 exons and spanning ~52 kb, with all of the introns conforming to the GT/AG rule. The mouse *Sptrx-2* gene maps at chromosome 13A3.3 between markers D13Mit154 and D13Mit79, very close to the mouse *Sfrp4* locus (60), although running in the opposite direction (Fig. 2). The rat *Sptrx-2* gene is also found in close proximity to the rat *Sfrp4* locus, which has been map at chromosome 17q12.1. These positions are syntenic with that of the human gene at chromosome 7p14.1 (9).

Murine Sptrx-2 mRNA Is Exclusively Expressed in the Testis—Multiple-tissue Northern blots were used to determine the size and tissue distribution of mouse *Sptrx-2* mRNA using the open reading frame as a probe. Mouse *Sptrx-2* mRNA was detected in the testis only as a single band of ~2.5 kb (Fig. 3*A*), which is in good agreement with the size of the cloned cDNA plus addition of the poly(A)$^+$ tail (GenBank^{TM}/EBI accession number AF548543). In contrast to our findings on human *SPTRX-2* mRNA (9), mouse RNA blots did not require as long an exposure time to identify a hybridization signal of comparable intensity. To evaluate the possibility that mouse *Sptrx-2* mRNA could be expressed during fetal development or in other tissues, we also screened an RNA dot blot containing poly(A)$^+$ RNA from 18 adult tissues and four fetal stages. Of the tissues examined, a hybridization signal was observed only in the testicular mRNA (Fig. 3*B*). To further investigate the expression pattern of murine *Sptrx-2* mRNA, *in situ* hybridization was performed in mouse and rat testicular sections. Mouse *Sptrx-2* mRNA was first detected in some (but not all) seminiferous tubules of testes from 3-week-old mice, whereas the vast majority of the tubules from 4-week-old or adult mice were labeled. In contrast, testes from 2-week-old pre-pubertal mice were not labeled and neither were the control sections of adult liver (Fig. 3*C*). Similarly, analysis of adult rat testicular sections showed strong labeling in all seminiferous tubules (Fig. 3*D*). In dipped sections of mouse testis, a strong signal was seen in the middle part of the seminiferous epithelium (Fig. 3*E*). At higher magnification, the strongest labeling corresponded to round spermatids, with a low-to-moderate signal in late primary spermatocytes and secondary spermatocytes (Fig. 3*F*). No signal was evident in the remaining testicular tissue or when control probes were used. This expression pattern is consistent with the *in situ* data reported for human *SPTRX-2* mRNA (9).

SPTRX-2 Protein Is Expressed during the Final Steps of Spermiogenesis—We have previously determined that human SPTRX-2 protein is mostly expressed in round and elongating spermatid stages of spermatogenesis (9). However, the temporal sequence of expression was difficult to determine at the histological level because of the intermingling of stages within the human seminiferous tubular cross-sections. Therefore, we performed a detailed SPTRX-2 expression analysis in rat and mouse testicular sections, in which the stages of the seminiferous epithelium are easily discernible within each seminiferous tubular cross-section. As shown in Fig. 4*A*, SPTRX-2 immunostaining became prominent in the cytoplasmic lobe of step 15 spermatids in stage I of the seminiferous epithelium cycle

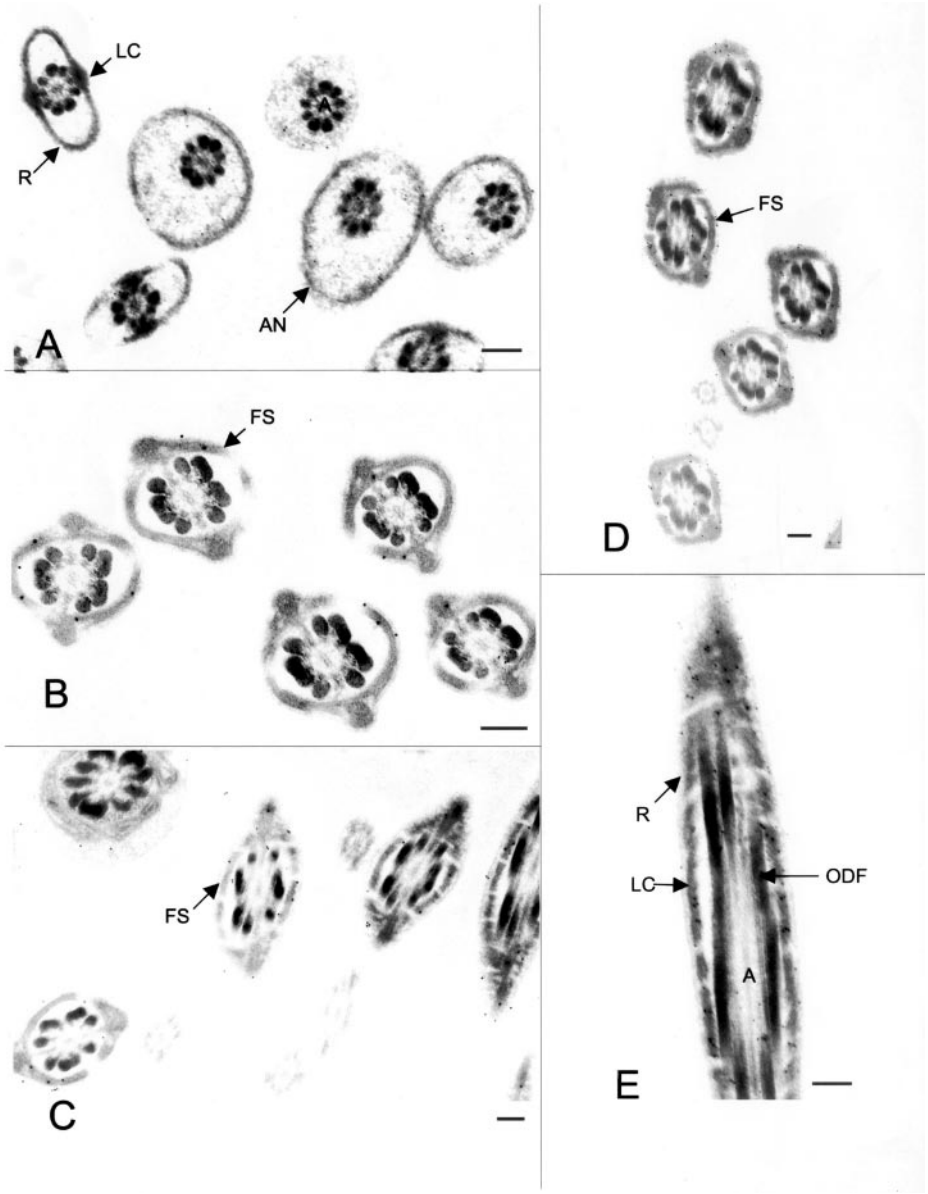

FIG. 6. **Electron micrographs of the sperm tail sections in steps 15–19 spermatids at stages I–VII of the cycle of the rat seminiferous epithelium, immunogold-labeled with anti-SPTRX-2 antibody.** In step 15 (*A*), labeling was scattered throughout the cytoplasm of the tail, whereas little was found on the FS anlagen (*AN*), ribs (*R*), or longitudinal columns (*LC*) of the FS. Incorporation of the label into the FS began in step 16 (*B*) and gradually increased through steps 17 and 18 (*C*) to reach a peak by step 19 (*D*). The oblique section through the principal piece of step 19 spermatids (*E*) shows the label to be interspersed throughout the longitudinal columns and ribs of the FS; little labeling was found in the axoneme (*A*) and ODFs at this late step. *Bars* = 0.2 μm.

(see Fig. 10 for orientation of rat spermatid steps), remained so until step 18, and diminished in step 19. On the other hand, tail immunoreactivity gradually increased through steps 15–18 and peaked in step 19 spermatids. By step 19 (stage VII), it was evident that immunoperoxidase labeling was confined to the distal part of the tail, *i.e.* the principal piece (Fig. 4*B*). Preincubation of anti-SPTRX-2 antibody with recombinant SPTRX-2 eliminated the immunostaining (Fig. 4*C*) and hence confirmed the specificity of the immunoreactivity of antibodies raised against human SPTRX-2 in rat testicular tubular sections. Mouse testis showed an expression pattern similar to that in rat testis (data not shown).

SPTRX-2 Is Incorporated into the Spermatid FS and Is an Integral FS Component of Mature Spermatozoa—To identify those structures in the developing spermatid tail with which SPTRX-2 associates, immunofluorescence microscopy was first performed on mouse testis and epididymal spermatozoa. As shown in Fig. 5 (*A–C*), SPTRX-2 was readily detectable in late spermatids in mouse testicular tissue sections, similar to the rat developmental analysis described above. In mouse epididymal sections, SPTRX-2 was found in the tails of spermatozoa (Fig. 5, *D* and *E*), and isolated spermatozoa clearly showed labeling in the tail principal piece compatible with localization to the FS (Fig. 5, *F–H*). During epididymal transit, SPTRX-2 was also found in the cytoplasmic droplet before and after it was shed from the distal mid-piece of the tail (Fig. 5, *F* and *H*) in what appears to be a common route for elimination of residual FS proteins (77). Pre-absorbed antibody with the recombinant protein was used as a negative control and demonstrated the specificity of the labeling (Fig. 5, *I* and *J*).

To characterize in detail the developmental localization of SPTRX-2, a complete survey of the spermatid steps was carried out by immunogold electron microscopy of the rat testicular tissue sections (Fig. 6, *A–E*). Immunogold labeling first appeared in the tails of steps 14 and 15 spermatids and was randomly scattered throughout the cytoplasm of the axoneme (Fig. 6*A*). The development of the principal piece in these steps and earlier is characterized by the assembly of FS precursor material (FS anlagen). It assembles in a distal-to-proximal direction along the plasmalemma of the tail and precedes the assembly of the ribs and columns of the FS that follow in its wake (61). In these steps, neither the anlagen nor the more distally located mature FS was immunolabeled (Fig. 6*A*). From a structural point of view, the assembly of the FS is almost completed in step 16; and therefore, it is surprising that the

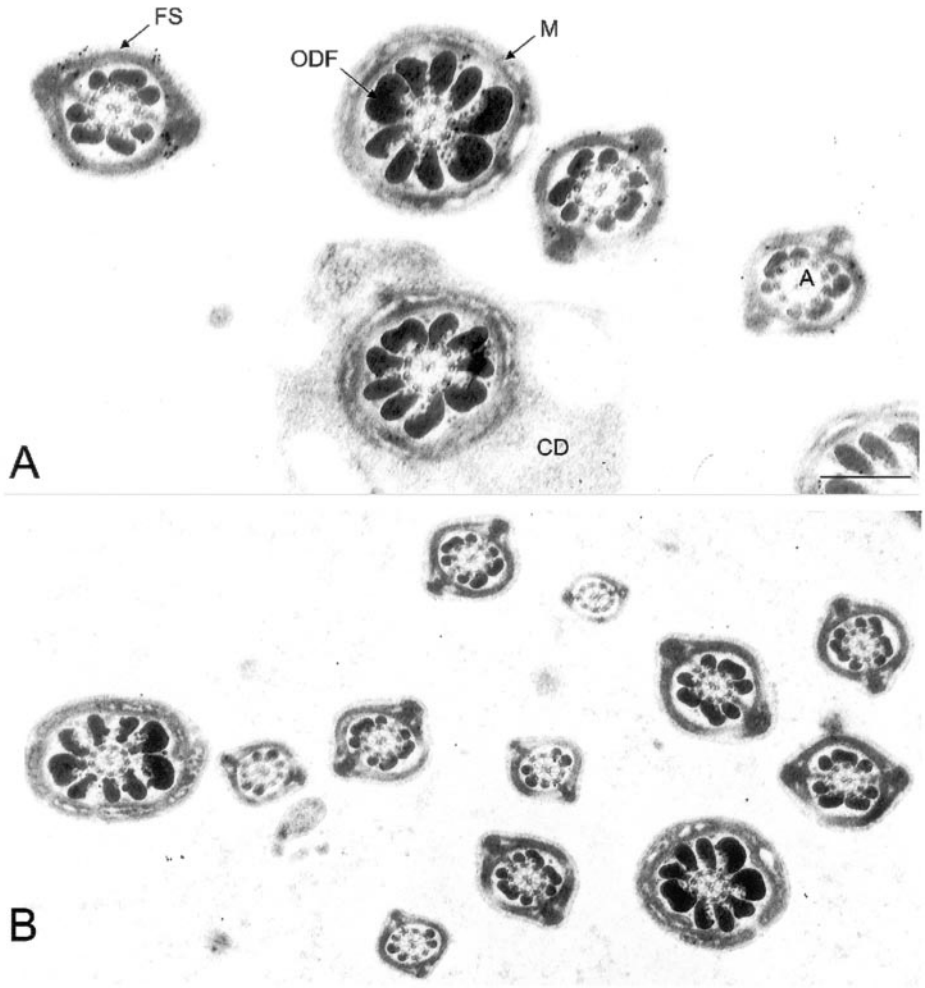

FIG. 7. **Electron micrographs of cauda epididymal sperm tails immunogold-labeled with anti-SPTRX-2 antibody (*A*) or with anti-SPTRX-2 antibody preincubated with recombinant SPTRX-2 (*B*).** Immunogold labeling was predominantly found over the FS. *M*, mitochondrial sheath; *A*, axoneme; *CD*, cyloplasmic droplet. *Bar* = 10 μm.

labeling first began to appear over the FS at this step of spermiogenesis (Fig. 6*B*). During steps 17 and 18, the immunogold labeling progressively increased over both the ribs and longitudinal columns of the FS, and a much lesser labeling was found free in the cytoplasmic lobe surrounding the flagellum (Fig. 6*C*). In step 19 spermatids, labeling of the FS reached its peak (Fig. 6*D*). From observing the immunolabeling of tangential sections through the principal piece at this step, it was apparent that SPTRX-2 was incorporated deeply through the ribs and longitudinal columns of the FS (Fig. 6*E*). Confirmation that SPTRX-2 is an integral component of the mature FS came from the analysis of spermatozoa in the cauda epididymis, where immunogold labeling of SPTRX-2 was found throughout the FS (Fig. 7*A*). Preincubation of anti-SPTRX-2 antibody with recombinant SPTRX-2 blocked this signal (Fig. 7*B*). Immunoblots of isolated FS from mature spermatozoa verified SPTRX-2 as an authentic constituent of the FS (Fig. 8). Interestingly, SPTRX-2 was resistant to extraction by urea under reducing conditions, a property of FS proteins that facilitates selective isolation of the FS from other sperm tail components.

Components of the sperm accessory structures (ODFs and FS) of mammalian spermatozoa are detected frequently as autoantigens in screens of sperm proteins with post-obstruction sera (62). Because rat SPTRX-2 was found to be a component of the FS, we asked whether it is recognized by antibodies in post-obstruction sera generated by performing vasectomies on rats (55). On two-dimensional Western blots of rat sperm extracts, the region between 65 and 84 kDa at pI ~5.0–5.7, where SPTRX-2 is expected to migrate, was strongly stained both by anti-SPTRX-2 serum (Fig. 9*A*) and by post-vasectomy

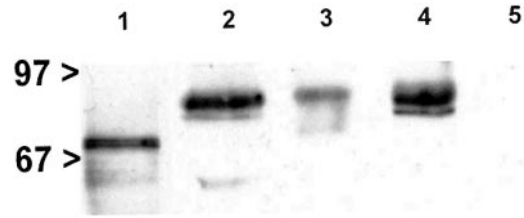

FIG. 8. **Western blot of denatured (under reducing conditions) and SDS-PAGE-run human recombinant SPTRX-2 (*lane 1*), whole rat sperm (*lane 2*), isolated rat sperm FS (*lane 3*), rat sperm tails (*lane 4*), and rat sperm heads (*lane 5*) probed with anti-SPTRX-2 antibody (diluted 1:1000).** Note that immunoreactivity was retained in isolated FS.

serum (Fig. 9*D*). Comigration of protein spots stained by anti-SPTRX-2 and post-vasectomy sera suggested that SPTRX-2 is an auto- and/or isoantigen in rats. To confirm this, Western blot analysis was conducted on one-dimensional polyacrylamide gels of human recombinant SPTRX-2 protein (Fig. 9, *C* and *F*). Anti-SPTRX-2 and post-vasectomy sera both reacted with a recombinant protein band at 68 kDa as well as with bands at lower molecular masses that are believed to be breakdown products of SPTRX-2. When blots of recombinant SPTRX-2 were stained with a panel of 13 post-vasectomy rat sera, 9 of the 13 sera (69%) showed a positive reaction: four bound a 68-kDa protein; two reacted with bands at 68 and 17 kDa; and five stained the putative breakdown product of 17 kDa.

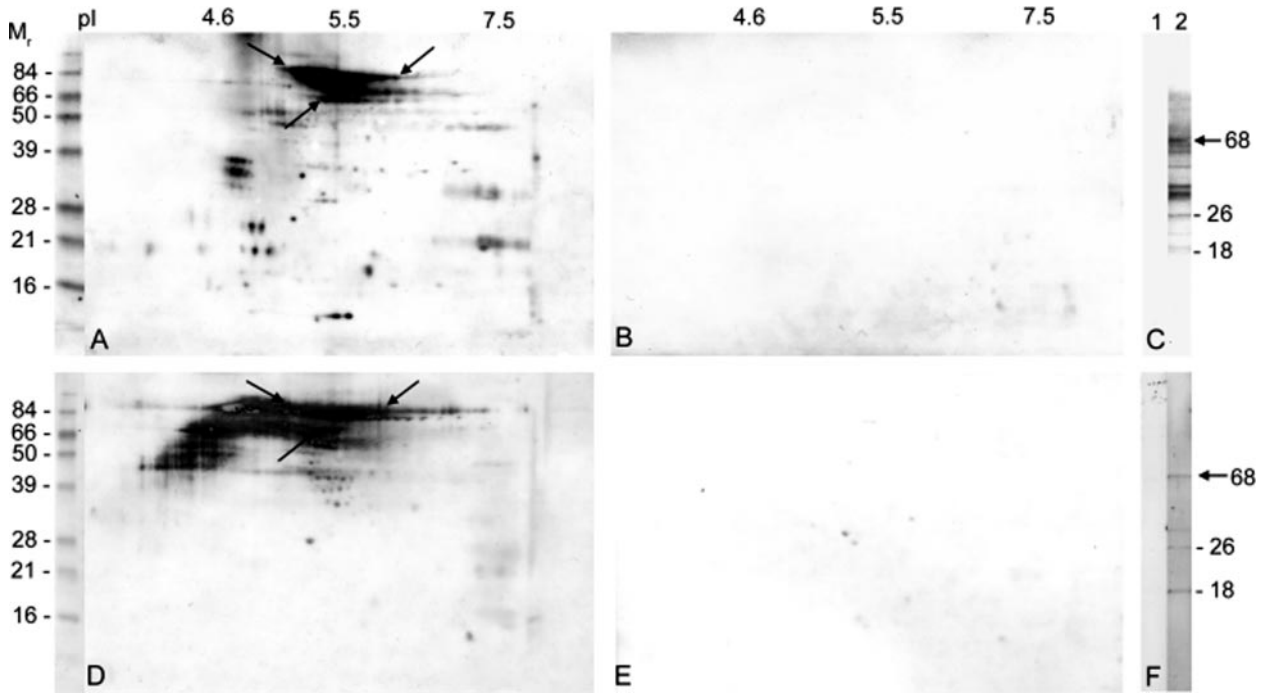

FIG. 9. **Identification of SPTRX-2 as a sperm autoantigen.** Shown are Western blots of rat sperm extracts stained with affinity-purified rabbit anti-SPTRX-2 antibody (*A* and *C*) or with a representative post-vasectomy rat serum (*D* and *F*). The *arrows* indicate groups of protein spots stained with anti-SPTRX-2 serum (*A*) that comigrated with sperm proteins bound by post-vasectomy serum (*D*), including the region between 65 and 75 kDa at pI 5.0–5.7, where sperm SPTRX-2 is expected to migrate. *C* and *F* show staining of a one-dimensional blot of recombinant SPTRX-2 protein with the identical sera used for *A* and *D*, respectively. Note that the post-vasectomy serum (*F*) stained a recombinant protein band at ~68 kDa, as did anti-SPTRX-2 serum (*C*). The bands at 26 and 18 kDa are believed to represent breakdown products of SPTRX-2. The preimmune anti-SPTRX-2 serum (*B* and *C*, *lane 1*) and the pre-vasectomy serum (*E* and *F*, *lane 1*) showed little reactivity.

DISCUSSION

We recently reported that human SPTRX-2, a protein composed of thioredoxin and NDP kinase domains, is present only in male germ cells (9). To determine its specific subcellular localization, we cloned both mouse and rat testicular *Sptrx-2* cDNAs and performed a detailed developmental study in the testes and spermatozoa of these two organisms, which identified SPTRX-2 as an integral component of the sperm FS. Murid *Sptrx-2* mRNA is exclusively expressed in the testis, mainly in round spermatids; it is restricted to the post-pubertal testis as shown by the absence of corresponding transcripts in 2-week-old testis, but presence in 3-week-old testicular tissue sections. This expression pattern follows that of other FS mRNAs such as FS39 and FS75 (35, 46), which are synthesized in round spermatids, stored for several days and translated in elongating spermatids following the termination of transcription, which occurs during nuclear condensation (63).

The murid SPTRX-2 protein has a domain organization identical to that of its human counterpart (9): an N-terminal thioredoxin domain followed by three NDP kinase domains, the first of which is incomplete, lacking the typical active site of this class of enzymes. Interestingly, this domain organization is found not only in mammals, but also in lower organisms such as the intermediate chain-1 protein from the sea urchin sperm axoneme (64) and the ascidian *Ciona intestinalis* intermediate chain-3 flagellar protein (65). In contrast, a search of animal model data bases including *Drosophila* and zebrafish failed to identify the corresponding orthologs. Moreover, whereas these proteins are part of the flagellum axoneme in sea urchins and ascidians, mammalian SPTRX-2 is located in the FS, a cytoskeletal structure that envelopes the sperm axoneme. It is thus tempting to speculate that, during evolution, the SPTRX-2 ancestor shifted from an axonemal to a periaxonemal localization. Because we have recently identified another protein in human axonemal structures (sperm flagella and lung cilia) that is composed of one N-terminal thioredoxin domain followed by only one NDP kinase domain, it is possible that this protein might substitute functionally for the SPTRX-2 ancestor in the axoneme (10). Such an axonemal-to-FS transition has been proposed recently due to the fact that the *DnaHc8* gene, which codes for a mouse testis-specific axonemal dynein heavy chain, might also code for an unusual isoform that could play a role in FS morphogenesis (66).

In addition to the axoneme, the mammalian sperm tail contains unique structural components such as ODFs and FS, which are synthesized during spermiogenesis and are involved in the regulation of sperm motility (14). By electron microscopic immunocytochemistry, we have determined that SPTRX-2 is an integral component of the sperm FS. Fig. 10 illustrates the expression pattern of SPTRX-2 during spermiogenesis in comparison with the pattern found for the majority of sperm FS proteins to date (14, 35, 77), including the transiently expressed thioredoxin SPTRX-1 (50). As shown, SPTRX-2 is incorporated into the FS after the bulk of FS proteins have already assembled to form it. Interestingly, the incorporation of SPTRX-2 into the FS during steps 17–19 is concomitant with the gradual disappearance of SPTRX-1 from the longitudinal columns of the FS. This replacement of one thioredoxin for another in the FS indicates a specific developmental/maturational function for each of these thioredoxins. Equally intriguing is that the FS has the appearance of a very electron-dense structure by step 17, yet is still penetrable by proteins. In this context, it is possible that not until the incorporation of SPTRX-2 into the FS is intensive disulfide bonding of this structure initiated. Alternatively, the S–S cross-linking could be delayed even further after SPTRX-2 incorporation into the FS and could occur during final sperm maturation in the epididymis.

Protein spots stained by anti-SPTRX-2 and post-vasectomy rat sera comigrated on two-dimensional Western blots of sperm

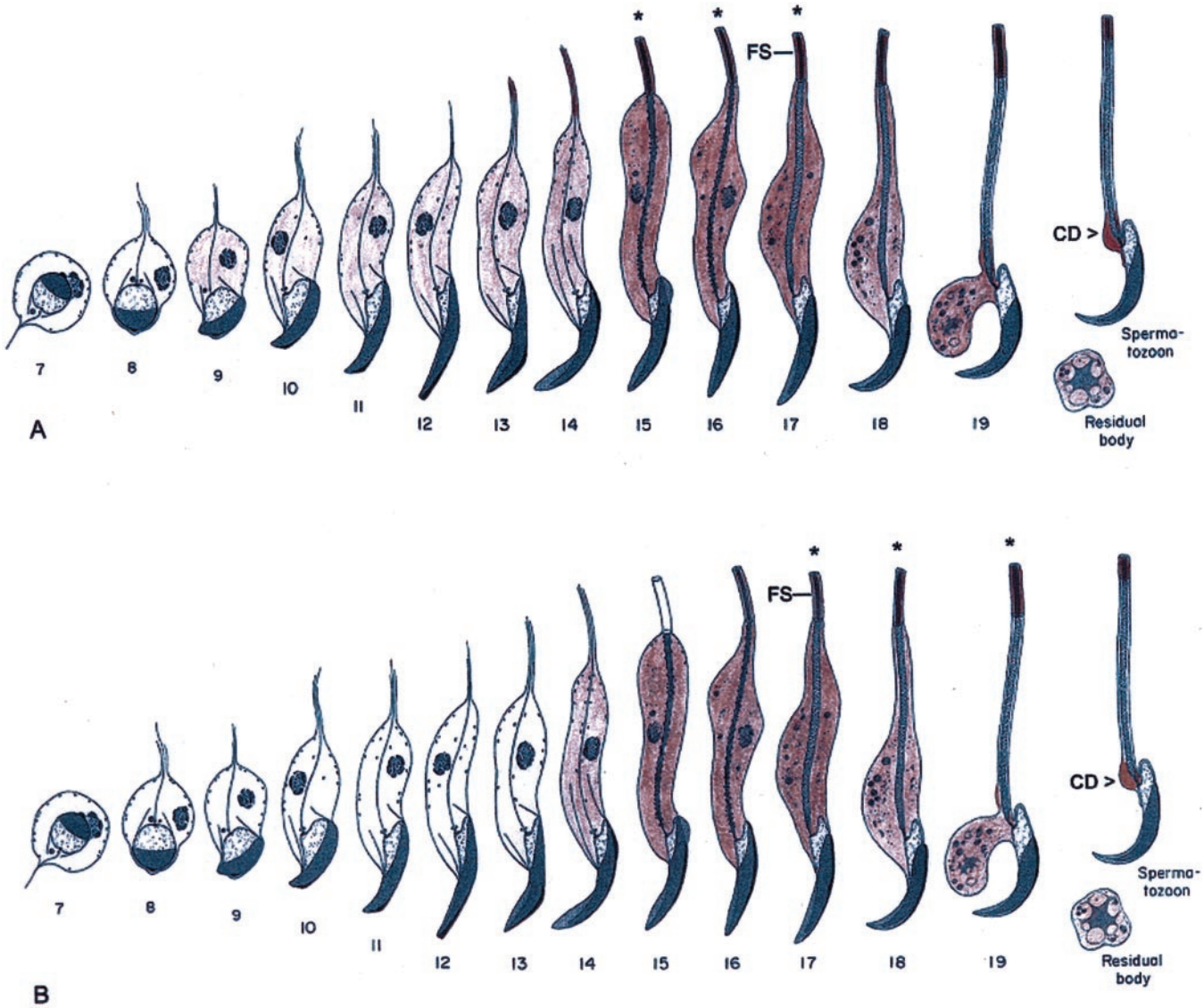

FIG. 10. **Comparison between the expression pattern of known FS proteins and SPTRX-2.** *A*, schematic presentation of rat spermiogenesis, adapted from Oko and Clermont (77), providing a summary of the areas and intensity of immunolabeling with antibodies raised against prominent FS proteins. The peak of assembly and cytoplasmic reactivity for FS proteins is in steps 15–17 (stages I–V), shown by *asterisks*. The structural assembly of the FS is complete by step 17. *B*, immunolabeling with anti-SPTRX-2 antibody shows the same peak of cytoplasmic reactivity as indicated above with the other FS proteins; however, maximum incorporation of SPTRX-2 into the structurally mature FS occurs during steps 17–19 (see *asterisks*). Comparatively, the incorporation of SPTRX-2 lags far behind the assembly of the majority of FS proteins. *CD*, cytoplasmic droplet.

extracts, and identification of SPTRX-2 as an autoantigen was subsequently confirmed by demonstrating that post-vasectomy rat serum bound recombinant SPTRX-2. Several characteristics of SPTRX-2 may be related to its antigenicity in vasectomized animals. Like other proteins expressed only during spermatogenesis, SPTRX-2 may be autoantigenic because it is not produced until after puberty, thus avoiding identification as a self-protein during the earlier development of the immune system (67). In addition, SPTRX-2 is associated with the FS, and components of the sperm cytoskeleton such as the ODFs are known to be prominent post-obstruction autoantigens (62), perhaps because the cytoskeleton is among the most degradation-resistant components of spermatozoa after obstruction, thus furnishing a supply of slowly released antigen to stimulate the immune system.

Both thioredoxins and NDP kinases are regarded as catalytic molecules, the first one being involved in redox reactions as a general disulfide reductase (1) and the second one catalyzing the transfer of γ-phosphates between nucleoside and deoxynucleoside di- and triphosphates (68). Surprisingly, we have not been able to detect any thioredoxin or NDP kinase enzymatic activity using recombinant SPTRX-2 expressed in bacteria (9). To our knowledge, neither activity has been detected in isolated sea urchin and ascidian intermediate chain-1 proteins (64, 65), suggesting that additional factors are required.

Although the thioredoxins are traditionally regarded to be general protein-disulfide reductases (1), disulfide bond formation (rather than reduction) is a major requirement for the stabilization of the different components of the cytoskeletal structures that provide the scaffolding for the sperm head and tail skeleton (69). The presence of two novel thioredoxins (SPTRX-1 and SPTRX-2) that are associated with the sperm FS at different times during its assembly raises important questions regarding the requirement of this class of proteins in spermiogenesis. We have recently reported that recombinant SPTRX-1 can act both as a reducing and an oxidizing protein (8, 70). This may facilitate the formation of disulfide bonds among individual components of the FS as well as destabilize

the misfolded and/or improperly incorporated sperm tail proteins. However, we have not been able to demonstrate any thioredoxin-dependent activity (either reducing or oxidizing) using recombinant SPTRX-2. Several reasons might account for this lack of activity *in vitro*, such as the requirement for additional cofactors not present in bacteria, post-translational modifications that might expose the active site upon conformational changes, etc. Nevertheless, given its FS localization and expression pattern during spermiogenesis, it is reasonable to speculate that SPTRX-2 might play a crucial role in disulfide bonding within the FS.

It is also conceivable that, although SPTRX-1 may fulfill a transitional function in sperm flagellar differentiation/biogenesis during spermiogenesis (50), SPTRX-2 may be necessary for post-testicular events such as epididymal sperm maturation, hyperactivation/capacitation, or even fertilization and zygotic development. In this regard, we have shown previously that the sperm tail FS, where SPTRX-2 resides, is one of the first sperm structures to be degraded in the zygotic cytoplasm upon fertilization. Solubilization of the FS precedes the degradation of paternal mitochondria and ODFs and coincides with the early stages of male pronuclear development (71). Extensive studies demonstrated the requirement of disulfide bond reduction for the successful processing of the sperm nucleus and sperm accessory structures during mammalian fertilization (72), and SPTRX-2 might help in regulating this process.

Furthermore, although we could not detect any kinase activity with recombinant SPTRX-2, its well conserved NDP kinase domain supports the idea that SPTRX-2 could be a phosphate donor for the phosphorylation of other FS proteins. Phosphorylation is the major regulatory mechanism in spermatozoa and underlies important processes during the acquisition of fertilizing capability by the spermatozoon, such as capacitation and hyperactivation (73). Interestingly, the major protein in the sperm FS is AKAP4, whose proposed function is to recruit/anchor protein kinase A to the FS to facilitate phosphorylation of proteins that regulate sperm flagellar motility (74). SPTRX-2 has several potential sites of phosphorylation by protein kinase A and other kinases and could be associated with the scaffold formed by AKAP4 and structural proteins of the sperm FS. The recent characterization of the mouse AKAP4 knockout phenotype suggests that AKAP4 does not affect the initial formation of the longitudinal columns and connecting ribs that characterize the mature FS, but AKAP4 does affect later steps of its assembly, leading to incomplete FS development (74). In this context, SPTRX-2 could then be incorporated into the fully differentiated FS as an associated protein of AKAP4, which remains in the mature FS and might play a role in later events undergone by the sperm by virtue of its proposed thioredoxin/kinase activity.

Acknowledgments—The skillful technical assistance of Miriam Sutovsky, Ulla Jukarainen, and Leigh Ann Bush is gratefully acknowledged.

REFERENCES

1. Arner, E. S., and Holmgren, A. (2000) *Eur. J. Biochem.* **267,** 6102–6109
2. Wollman, E. E., d'Auriol, L., Rimsky, L., Shaw, A., Jacquot, J. P., Wingfield, P., Graber, P., Dessarps, F., Robin, P., and Galibert, F. (1988) *J. Biol. Chem.* **263,** 15506–15512
3. Damdimopoulos, A. E., Miranda-Vizuete, A., Pelto-Huikko, M., Gustafsson, J.-Å., and Spyrou, G. (2002) *J. Biol. Chem.* **277,** 33249–33257
4. Miranda-Vizuete, A., Gustafsson, J.-Å., and Spyrou, G. (1998) *Biochem. Biophys. Res. Commun.* **243,** 284–288
5. Lee, K.-K., Murakawa, M., Takahashi, S., Tsubuki, S., Kawashima, S., Sakamaki, K., and Yonehara, S. (1998) *J. Biol. Chem.* **273,** 19160–19166
6. Hosoda, A., Kimata, Y., Tsuru, A., and Kohno, K. (2003) *J. Biol. Chem.* **278,** 2669–2676
7. Cunnea, P. M., Miranda-Vizuete, A., Bertoli, G., Simmen, T., Damdimopoulos, A. E., Hermann, S., Leinonen, S., Huikko, M. P., Gustafsson, J.-Å., Sitia, R., and Spyrou, G. (2003) *J. Biol. Chem.* **278,** 1059–1066
8. Miranda-Vizuete, A., Ljung, J., Damdimopoulos, A. E., Gustafsson, J.-Å., Oko, R., Pelto-Huikko, M., and Spyrou, G. (2001) *J. Biol. Chem.* **276,** 31567–31574
9. Sadek, C. M., Damdimopoulos, A. E., Pelto-Huikko, M., Gustafsson, J.-Å., Spyrou, G., and Miranda-Vizuete, A. (2001) *Genes Cells* **6,** 1077–1090
10. Sadek, C. M., Jimenez, A., Damdimopoulos, A. E., Kieselbach, T., Nord, M., Gustafsson, J.-Å., Spyrou, G., Davis, E. C., Oko, R., van der Hoorn, F. A., and Miranda-Vizuete, A. (2003) *J. Biol. Chem.* **278,** 13133–13142
11. Nordberg, J., and Arner, E. S. (2001) *Free Radic. Biol. Med.* **31,** 1287–1312
12. Powis, G., and Montfort, W. R. (2001) *Annu. Rev. Pharmacol. Toxicol.* **41,** 261–295
13. Curry, M. R., and Watson, P. F. (1995) in *Gametes: The Spermatozoon* (Grudzinskas, J. G., and Yovich, J. L., eds) pp. 45–69, University of Cambridge, Cambridge
14. Oko, R. (1998) *Andrologia* **30,** 193–206
15. Oko, R., Aul, R. B., Wu, A., and Sutovsky, P. (2001) in *Andrology in the 21st Century* (Robaire, B., Chemes, H., and Morales, C. R., eds) pp. 37–45, Medical Publications, Medimond, NJ
16. Aul, R. B., and Oko, R. J. (2002) *Dev. Biol.* **242,** 376–387
17. Sutovsky, P., Manandhar, G., and Oko, R. (2003) *Microsc. Res. Tech.* **61,** 362–378
18. Fawcett, D. W. (1975) *Dev. Biol.* **44,** 394–436
19. Eddy, E. M., Toshimori, K., and O'Brien, D. A. (2003) *Microsc. Res. Tech.* **61,** 103–115
20. Baltz, J. M., Williams, P. O., and Cone, R. A. (1990) *Biol. Reprod.* **43,** 485–491
21. Williams, A. C., and Ford, W. C. (2001) *J. Androl.* **22,** 680–695
22. Tash, J. S., and Bracho, G. E. (1994) *J. Androl.* **15,** 505–509
23. Feliciello, A., Gottesman, M. E., and Avvedimento, E. V. (2001) *J. Mol. Biol.* **308,** 99–114
24. Burfeind, P., and Hoyer-Fender, S. (1991) *Dev. Biol.* **148,** 195–204
25. Morales, C. R., Oko, R., and Clermont, Y. (1994) *Mol. Reprod. Dev.* **37,** 229–240
26. van der Hoorn, F. A., Tarnasky, H. A., and Nordeen, S. K. (1990) *Dev. Biol.* **142,** 147–154
27. Brohmann, H., Pinnecke, S., and Hoyer-Fender, S. (1997) *J. Biol. Chem.* **272,** 10327–10332
28. Schalles, U., Shao, X., van der Hoorn, F. A., and Oko, R. (1998) *Dev. Biol.* **199,** 250–260
29. Shao, X., Tarnasky, H. A., Schalles, U., Oko, R., and van der Hoorn, F. A. (1997) *J. Biol. Chem.* **272,** 6105–6113
30. Petersen, C., Aumuller, G., Bahrami, M., and Hoyer-Fender, S. (2002) *Mol. Reprod. Dev.* **61,** 102–112
31. O'Bryan, M. K., Sebire, K., Meinhardt, A., Edgar, K., Keah, H. H., Hearn, M. T., and De Kretser, D. M. (2001) *Mol. Reprod. Dev.* **58,** 116–125
32. Tres, L. L., and Kierszenbaum, A. L. (1996) *Mol. Reprod. Dev.* **44,** 395–407
33. Carrera, A., Gerton, G. L., and Moss, S. B. (1994) *Dev. Biol.* **165,** 272–284
34. Carrera, A., Moos, J., Ning, X. P., Gerton, G. L., Tesarik, J., Kopf, G. S., and Moss, S. B. (1996) *Dev. Biol.* **180,** 284–296
35. El-Alfy, M., Moshonas, D., Morales, C. R., and Oko, R. (1999) *J. Androl.* **20,** 307–318
36. Fulcher, K. D., Mori, C., Welch, J. E., O'Brien, D. A., Klapper, D. G., and Eddy, E. M. (1995) *Biol. Reprod.* **52,** 41–49
37. Turner, R. M., Musse, M. P., Mandal, A., Klotz, K., Jayes, F. C., Herr, J. C., Gerton, G. L., Moss, S. B., and Chemes, H. E. (2001) *J. Androl.* **22,** 302–315
38. Visconti, P. E., Johnson, L. R., Oyaski, M., Fornes, M., Moss, S. B., Gerton, G. L., and Kopf, G. S. (1997) *Dev. Biol.* **192,** 351–363
39. Mandal, A., Naaby-Hansen, S., Wolkowicz, M. J., Klotz, K., Shetty, J., Retief, J. D., Coonrod, S. A., Kinter, M., Sherman, N., Cesar, F., Flickinger, C. J., and Herr, J. C. (1999) *Biol. Reprod.* **61,** 1184–1197
40. Mei, X., Singh, I. S., Erlichman, J., and Orr, G. A. (1997) *Eur. J. Biochem.* **246,** 425–432
41. Fulcher, K. D., Welch, J. E., Klapper, D. G., O'Brien, D. A., and Eddy, E. M. (1995) *Mol. Reprod. Dev.* **42,** 415–424
42. Bunch, D. O., Welch, J. E., Magyar, P. L., Eddy, E. M., and O'Brien, D. A. (1998) *Biol. Reprod.* **58,** 834–841
43. Mori, C., Nakamura, N., Welch, J. E., Gotoh, H., Goulding, E. H., Fujioka, M., and Eddy, E. M. (1998) *Mol. Reprod. Dev.* **49,** 374–385
44. Fujita, A., Nakamura, K., Kato, T., Watanabe, N., Ishizaki, T., Kimura, K., Mizoguchi, A., and Narumiya, S. (2000) *J. Cell Sci.* **113,** 103–112
45. Nakamura, K., Fujita, A., Murata, T., Watanabe, G., Mori, C., Fujita, J., Watanabe, N., Ishizaki, T., Yoshida, O., and Narumiya, S. (1999) *FEBS Lett.* **445,** 9–13
46. Catalano, R. D., Hillhouse, E. W., and Vlad, M. (2001) *Biol. Reprod.* **65,** 277–287
47. Naaby-Hansen, S., Mandal, A., Wolkowicz, M. J., Sen, B., Westbrook, V. A., Shetty, J., Coonrod, S. A., Klotz, K. L., Kim, Y. H., Bush, L. A., Flickinger, C. J., and Herr, J. C. (2002) *Dev. Biol.* **242,** 236–254
48. Egydio de Carvalho, C., Tanaka, H., Iguchi, N., Ventela, S., Nojima, H., and Nishimune, Y. (2002) *Biol. Reprod.* **66,** 785–795
49. Nakamura, Y., Tanaka, H., Koga, M., Miyagawa, Y., Iguchi, N., Egydio de Carvalho, C., Yomogida, K., Nozaki, M., Nojima, H., Matsumiya, K., Okuyama, A., and Nishimune, Y. (2002) *Biol. Reprod.* **67,** 1–7
50. Yu, Y., Oko, R., and Miranda-Vizuete, A. (2002) *Biol. Reprod.* **67,** 1546–1554
51. Altschul, S. F., and Koonin, E. V. (1998) *Trends Biochem. Sci.* **23,** 444–447
52. Kononen, J., and Pelto-Hiukko, M. (1997) *Technical Tips Online* http://tto.trends.com/
53. Oko, R. J., Jando, V., Wagner, C. L., Kistler, W. S., and Hermo, L. S. (1996) *Biol. Reprod.* **54,** 1141–1157
54. Leblond, C., and Clermont, Y. (1952) *Am. J. Anat.* **90,** 167–215
55. Flickinger, C. J., Bush, L. A., Williams, M. V., Naaby-Hansen, S., Howards, S. S., and Herr, J. C. (1999) *J. Reprod. Immunol.* **43,** 35–53
56. Naaby-Hansen, S., Flickinger, C. J., and Herr, J. C. (1997) *Biol. Reprod.* **56,** 771–787
57. Laemmli, U. K. (1970) *Nature* **227,** 680–685
58. Bush, L. A., Herr, J. C., Wolkowicz, M., Sherman, N. E., Shore, A., and

Flickinger, C. J. (2002) *Mol. Reprod. Dev.* **62,** 233–247
59. Bairoch, A., Buchner, P., and Hofmann, K. (1997) *Nucleic Acids Res.* **25,** 217–221
60. Rattner, A., Hsieh, J. C., Smallwood, P. M., Gilbert, D. J., Copeland, N. G., Jenkins, N. A., and Nathans, J. (1997) *Proc. Natl. Acad. Sci. U. S. A.* **94,** 2859–2863
61. Clermont, Y., Oko, R., and Hermo, L. (1990) *Anat. Rec.* **227,** 447–457
62. Flickinger, C. J., Rao, J., Bush, L. A., Sherman, N. E., Oko, R. J., Jayes, F. C., and Herr, J. C. (2001) *Biol. Reprod.* **64,** 1451–1459
63. Kleene, K. C. (1996) *Mol. Reprod. Dev.* **43,** 268–281
64. Ogawa, K., Takai, H., Ogiwara, A., Yokota, E., Shimizu, T., Inaba, K., and Mohri, H. (1996) *Mol. Biol. Cell* **7,** 1895–1907
65. Padma, P., Hozumi, A., Ogawa, K., and Inaba, K. (2001) *Gene* (*Amst.*) **275,** 177–183
66. Samant, S., Ogunkua, O., Hui, L., Fossella, J., and Pilder, S. (2002) *Dev. Biol.* **250,** 24–43
67. Tung, K. S. K., and Menge, A. C. (1985) in *The Autoimmune Diseases* (Rose, N. R., and Mackay, I. R., eds) pp. 537–590, Academic Press, Inc., New York
68. Lombardi, D., Lacombe, M. L., and Paggi, M. G. (2000) *J. Cell. Physiol.* **182,** 144–149
69. Calvin, H. (1975) in *Biology of the Male Gamete* (Duckett, J. G., and Racey, P. A., eds) pp. 257–273, Academic Press, Inc., New York
70. Jimenez, A., Johansson, C., Ljung, J., Sagemark, J., Berndt, K. D., Ren, B., Tibbelin, G., Ladenstein, R., Kieselbach, T., Holmgren, A., Gustafsson, J.-Å., and Miranda-Vizuete, A. (2002) *FEBS Lett.* **530,** 79–84
71. Sutovsky, P., Navara, C. S., and Schatten, G. (1996) *Biol. Reprod.* **55,** 1195–1205
72. Sutovsky, P., and Schatten, G. (2000) *Int. Rev. Cytol.* **195,** 1–65
73. Yanagimachi, R. (1994) in *The Physiology of Reproduction* (Knobil, E., and Neill, J. D., eds) pp. 189–317, Raven Press, Ltd., New York
74. Miki, K., Willis, W. D., Brown, P. R., Goulding, E. H., Fulcher, K. D., and Eddy, E. M. (2002) *Dev. Biol.* **248,** 331–342
75. Thompson, J. D., Higgins, D. G., and Gibson, T. J. (1994) *Nucleic Acids Res.* **22,** 4673–4680
76. Kong, A., Gudbjartsson, D. F., Sainz, J., Jonsdottir, G. M., Gudjonsson, S. A., Richardsson, B., Sigurdardottir, S., Barnard, J., Hallbeck, B., Masson, G., Shlien, A., Palsson, S. T., Frigge, M. L., Thorgeirsson, T. E., Gulcher, J. R., and Stefansson, K. (2002) *Nat. Genet.* **31,** 241–247
77. Oko, R., and Clermont, Y. (1989) *Anat. Rec.* **225,** 46–55

Cloning and Developmental Analysis of Murid Spermatid-specific Thioredoxin-2 (SPTRX-2), a Novel Sperm Fibrous Sheath Protein and Autoantigen

Antonio Miranda-Vizuete, Katie Tsang, Yang Yu, Alberto Jiménez, Markku Pelto-Huikko, Charles J. Flickinger, Peter Sutovsky and Richard Oko

J. Biol. Chem. 2003, 278:44874-44885.
doi: 10.1074/jbc.M305475200 originally published online August 7, 2003
